OPEN

Experimental & Molecular Medicine (2018) 50, e459; doi:10.1038/emm.2017.299
Official journal of the Korean Society for Biochemistry and Molecular Biology
www.nature.com/emm

ORIGINAL ARTICLE

HSP60 is required for stemness and proper differentiation of mouse embryonic stem cells

Nan-Hee Seo[1], Eun-Hye Lee[1], Jin-Hee Seo[1], Hwa-Ryung Song and Myung-Kwan Han

Embryonic stem cells (ESCs) are metabolically distinct from their differentiated counterparts. ESC mitochondria are less complex and fewer in number than their differentiated progeny. However, few studies have examined the proteins responsible for differences in mitochondrial structure and function between ESCs and somatic cells. Therefore, in this study, we aimed to investigate the differences between mitochondrial proteins in these two cell types. We demonstrate that HSP60 is more abundant in mouse ESC mitochondria than in mouse embryonic fibroblasts. Depletion of HSP60 inhibited mouse ESC proliferation and self-renewal, characterized by decreased OCT4 expression. HSP60 depletion also enhanced apoptosis during mouse ESC differentiation into embryoid bodies. Our results suggest that HSP60 expression has an essential role in ESC self-renewal and survival of differentiated cells from ESCs.
Experimental & Molecular Medicine (2018) **50,** e459; doi:10.1038/emm.2017.299; published online 16 March 2018

INTRODUCTION

Embryonic stem cells (ESCs) have the remarkable capacity to not only proliferate indefinitely but also generate any type of cell in the body.[1] Therefore, ESCs are thought to hold great promise for tissue repair and regeneration, and to provide a powerful tool for modeling human disease and understanding biological development.[2,3] However, to take advantage of the full potential of ESCs, it is critical to understand the mechanisms underlying the regulation of ESC self-renewal and differentiation.

ESC metabolism is distinct from that of their differentiated counterparts and has an important role in the maintenance of ESC identity.[4] ESCs have immature mitochondria with poorly developed cristae; upon differentiation, these immature mitochondria mature into mitochondria with dense matrix and complex cristae.[5,6] Consistent with these observations, ESCs rely on high rates of glycolysis, even when cultured *in vitro*. Upon differentiation, ESCs undergo a dramatic metabolic shift to oxidative phosphorylation.[6] Because of the immense therapeutic potential of human ESCs, a thorough understanding of the mechanisms by which human ESCs maintain their mitochondrial 'stemness' is crucial. However, few studies have examined which proteins are responsible for differences in mitochondrial structure and function between ESCs and somatic cells.

In this study, we used proteomic analysis to compare mitochondrial proteins between somatic cells and ESCs. Comparisons between mouse embryonic fibroblasts (MEFs) and mESCs revealed that levels of HSP60, vimentin and transitional endoplasmic reticulum ATPase were increased in mESCs relative to MEFs, whereas calnexin and ATP synthetase subunit-β levels were decreased in mESCs compared with MEFs. Notably, we found that depletion of HSP60 in ESCs inhibited proliferation and enhanced apoptosis levels during differentiation into embryoid bodies (EBs), indicating that HSP60 is a regulator of ESC stemness and differentiation.

MATERIALS AND METHODS

Cell culture and treatment

The mESC line Nagy R1 (Sigma, St. Louis, MO, USA) was maintained on 0.2% gelatin-coated plates in Dulbecco's modified Eagle's medium containing 15% fetal bovine serum, 1% GlutaMax (Gibco, Waltham, MA, USA), 1% non-essential amino acids (Gibco, Carlsbad, CA, USA), 100 U ml^{-1} penicillin, 100 U ml^{-1} streptomycin, 100 μM 2-mercaptoethanol and 1000 U ml^{-1} mouse recombinant leukemia inhibitory factor (Gibco, CA, USA).

Mitochondrial fractionations

mESCs and MEFs (2×10^7 cells) were collected, washed twice with phosphate-buffered saline and homogenized with 100 μl of lysis buffer consisting of 250 mM sucrose, 20 mM HEPES (pH 7.4), 10 mM KCl,

Department of Microbiology, Chonbuk National University Medical School, Jeonju, Republic of Korea
[1]These authors share first authorship.
Correspondence: Dr H-R Song or Professor M-K Han, Department of Microbiology, Chonbuk National University Medical School, Geonji-Ro 20, Jeonju, Jeonbuk 54896, Korea.
E-mail: silverysk@hanmail.net or iamtom@chonbuk.ac.kr
Received 30 May 2017; revised 12 September 2017; accepted 27 September 2017

1.5 mM Na-EGTA, 1.5 mM Na-EDTA, 1 mM $MgCl_2$, 1 mM dithiothreitol and 2 μg ml^{-1} aprotinin by passing the solution through a 27-gauge syringe 20 times. After homogenization, cells were centrifuged at 600 *g* for 10 min at 4 °C, to remove nuclei, unbroken cells and debris. Supernatants containing mitochondria were transferred to a new tube and were further centrifuged at 10 000 *g* for 10 min at 4 °C. Mitochondrial pellets were washed in 100 μl of lysis buffer followed by centrifugation at 10 000 *g* for 10 min at 4 °C.

Western blotting

Cells were lysed with M-PER mammalian protein extraction reagent (Pierce, Rockford, IL, USA) supplemented with a protease inhibitor cocktail (Roche, Indianapolis, IN, USA) and a phosphatase inhibitor cocktail (Roche), and were incubated on ice for 1 h. After centrifugation (10 000 *g* for 10 min), the cell lysates were separated by SDS-polyacrylamide gel electrophoresis (PAGE) and transferred to polyvinylidene difluoride membranes. The blots were incubated with anti-HSP60 (Santa Cruz Biotechnology, Dallas, TX, USA), anti-β-actin, anti-OCT4 anti-caspase 3 and anti-apoptosis-inducing factor (AIF) antibodies, and were subsequently incubated with goat anti-mouse or anti-rabbit alkaline phosphatase-conjugated secondary antibodies (Santa Cruz Biotechnology). The proteins were visualized using an enhanced chemiluminescence system (Intron, Seong-Nam, Republic of Korea) and an LAS 3000 imaging system (Fuji, Tokyo, Japan).

Immunofluorescence

The cells were grown on confocal dishes, fixed in 4% paraformaldehyde, washed with phosphate-buffered saline and then permeabilized with 0.1% Triton X-100. MitoTracker CMXRos Red (Invitrogen, Carlsbad, CA, USA) was used to stain mitochondria before fixation. The cells were stained with primary antibodies against HSP60, α-feto protein, brachyury and nestin (Santa Cruz Biotechnology) overnight at 4 °C. Cells were then stained with the appropriate secondary antibody, including Alexa Fluor 488 goat anti-mouse IgG, Alexa Fluor 594 donkey anti-rabbit IgG, Alexa Fluor 488 donkey anti-rabbit IgG or Alexa Fluor 594 donkey anti-mouse IgG (Invitrogen). Nuclei were stained with 4′,6-diamidino-2-phenylindole. Images were acquired using an Olympus IX71 fluorescence microscope with MetaMorph software (Molecular Devices, Sunnyvale, CA, USA).

Production of mESCs expressing HSP60 shRNA

shHSP60 was expressed using the inducible lentiviral vector pLKO-Tet-On (Addgene, Cambridge, MA, USA). The vector sequence encoding HSP60 short hairpin RNA (shRNA) is as follows: 5′-CCGGCACTGTTCT
GGCACGATCTCTCGAGAGATCGTGCCAGAACAGTGTTTTT-3′.
Non-targeting shRNA (pLKO-puro/non-targeting; Addgene) was used as a negative control. We produced viral particles in HEK293FT cells and used the viral particles to transduce R1 ESCs, which were subsequently cultured in the presence of 1 μg ml^{-1} puromycin. HSP60 expression was induced using 2 μg ml^{-1} doxycycline.

Small interfering RNA and transfection

For transient gene silencing, small interfering RNAs against AIF, small interfering RNA against HSP60 and non-targeting small interfering RNAs were purchased from Bioneer (Daejeon, Republic of Korea) and were transfected into cells for 48 h according to the manufacturer's instructions (Lipofectamine 2000; Invitrogen).

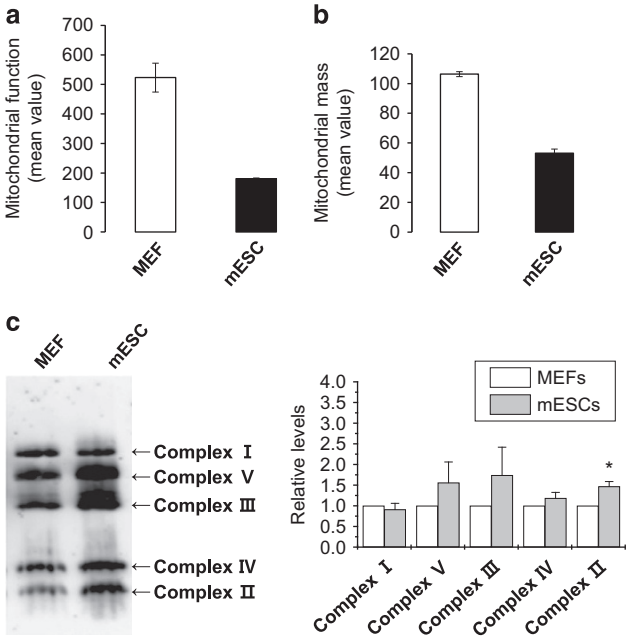

Figure 1 Comparison of mitochondrial function and respiratory complex levels between MEFs and mESCs. Mitochondrial function (**a**) and mass (**b**) in MEFs and mESCs. MEFs and mESCs were incubated with 2 μM 5,5′,6,6′-tetrachloro-1,1′3,3′-tetraethylbenzamidazol carboncyanine (JC-1) (**a**) or 10 μM 10-nonyl bromide (NAO) (**b**) for 30 min. JC-1 and NAO fluorescence were measured by flow cytometry at 480 and 550 nm, respectively. Data represent mean fluorescence ± s.d. (**c**) Separation of the mitochondrial respiratory complexes of MEFs and mESCs by blue-native gel electrophoresis. The positions of the complexes are indicated by Roman numerals on the right. The expression levels of the complexes were quantified based on the gel blot image by Fusion Fx7 and Fusion-Capt Advance software (Peqlab). The graph shows relative expression levels of the mitochondrial complexes between MEFs and mESCs. $^*P<0.01$.

Blue native PAGE and SDS-PAGE

Mitochondrial pellets were lysed with blue native buffer (20 mM Bis-Tris, 500 mM ε-aminocaproic acid, 20 mM NaCl, 2 mM EDTA 2, 10% glycerol and protease inhibitors) and 1% *n*-dodecyl β-D-maltoside at pH 7.0 and centrifuged at 20 000 *g* for 10 min. The supernatant was then collected for analysis by 5–15% blue native-PAGE. Duplicate lanes in the resulting blue native-PAGE were excised, equilibrated for 10 min at 70 °C and 20 min at room temperature in 2× SDS Laemmli loading buffer under reducing conditions and subjected to a second-dimension separation by 5–15% SDS-PAGE. The spots were analyzed by matrix-assisted laser desorption/ionization-time-of-flight mass spectrometry (Voyager-DE PRO, Waltham, MA, USA) for peptide mass fingerprinting and by electrospray ionization quadrupole time of flight mass spectrometry for peptide sequencing. Database searches were performed using MS-Fit, which can be accessed at http://prospector.uscf.edu.

Real-time PCR

HSP60 gene expression was examined by real-time PCR. Total RNA was prepared using an RNA extraction kit (Qiagen, Germantown, MD, USA). RNA samples were reverse transcribed with random primers using a reverse transcription system (Power cDNA Synthesis

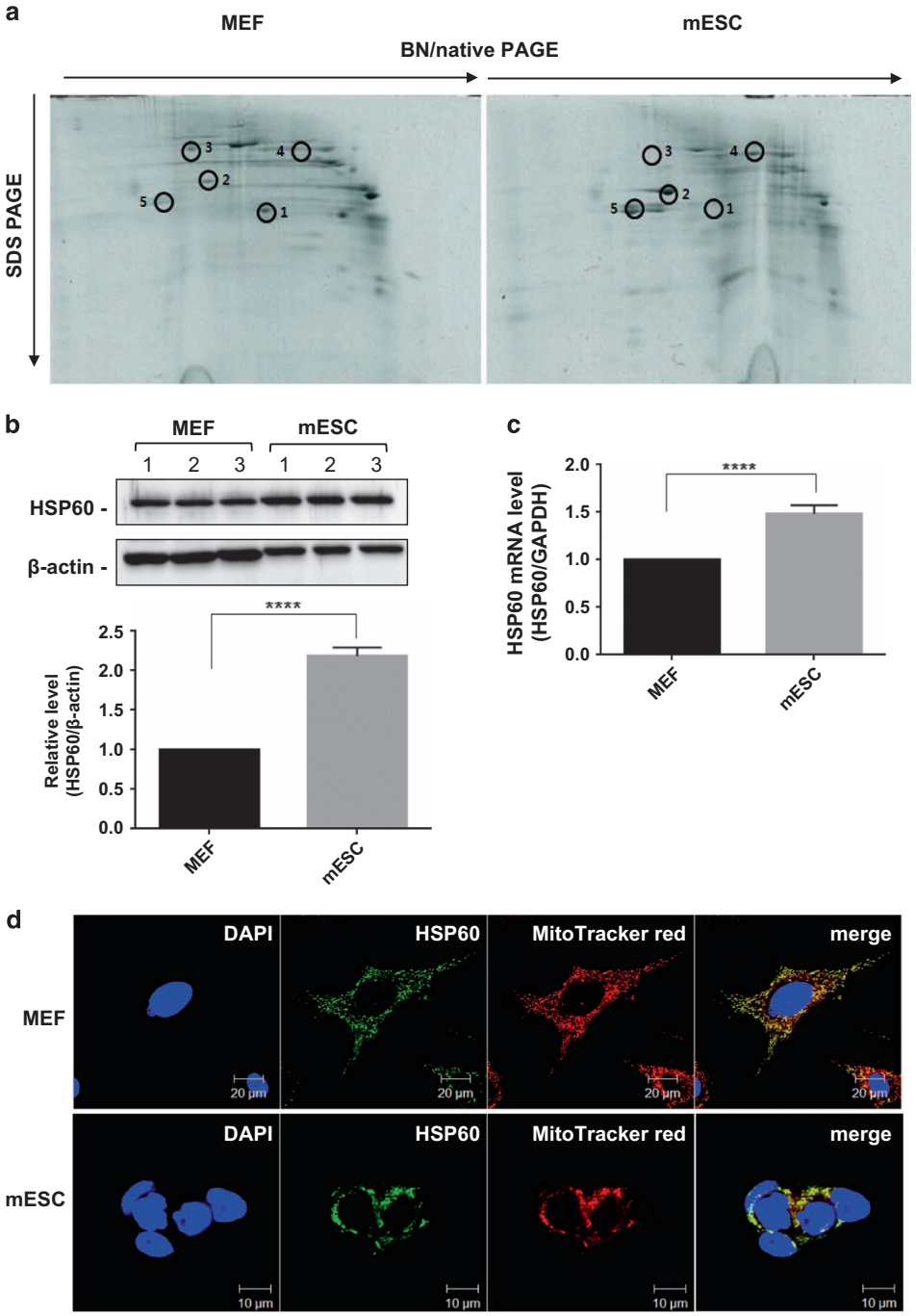

Figure 2 Increased expression of HSP60 in mESC mitochondria. (**a**) Two-dimensional resolution of the mitochondrial proteomes from MEFs and mESCs by blue-native/SDS-PAGE. Circles indicate the identified proteins. Identities of the separated protein complexes are as follows: (1) vimentin, (2) heat shock protein 60, (3) transitional endoplasmic reticulum ATPase, (4) calnexin and (5) ATP synthase subunit-β. (**b**) HSP60 protein expression in MEFs and mESCs. HSP60 protein levels were quantified based on the gel blot image by Fusion Fx7 and Fusion-Capt Advance software (Peqlab). Relative HSP60 band intensity was normalized to β-actin and quantified with respect to MEFs set to 1.0. The graph shows relative HSP60 expression levels between MEFs and mESCs. $*P<0.001$. (**c**) Relative HSP60 mRNA expression in MEFs and mESCs, calculated by normalization to GAPDH. (**d**) Mitochondrial localization of HSP60 in MEFs and mECSs. Cells were fixed, stained with anti-HSP60 antibody and visualized by indirect immunofluorescence. Mitochondria and nuclei were stained with MitoTracker Red and 4',6-diamidino-2-phenylindole, respectively.

Kit; Qiagen). Real-time PCR was performed using the C1000 thermal cycler (Bio Rad, Hercules, CA, USA) and SYBR Premix Ex Taq (Takara, Shiga, Japan). Quantification of *HSP60* expression levels was performed using the CFX96 Real-Time PCR Detection System (Bio Rad). Fold differences were calculated using the ΔCt method normalized to *Gapdh*.

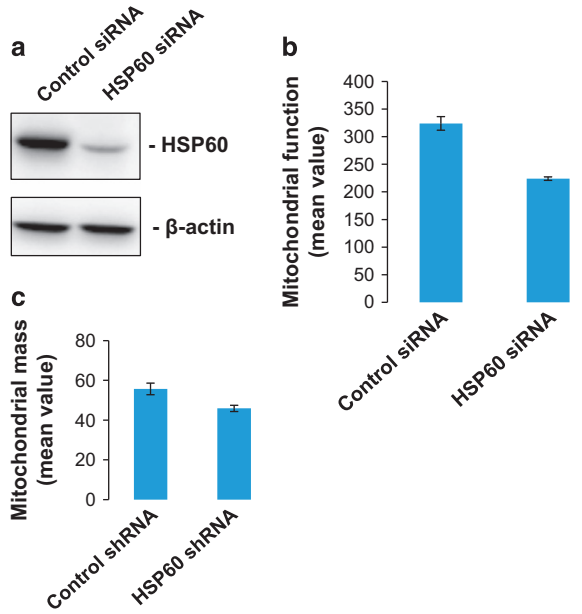

Figure 3 The effects of HSP60 knockdown on mitochondrial function and mass in mESCs. (**a**) HSP60 knockdown in mESCs using a doxycycline-inducible shRNA-expressing lentiviral vector. mESCs were infected with doxycycline-inducible control shRNA or HSP60 shRNA-expressing lentiviral vector and selected with puromycin. The cells were further treated with 10 μg ml^{-1} doxycycline for 3 days. Next, the cells were lysed and protein levels were determined by western blotting. Mitochondrial function (**b**) and mass (**c**) in MEFs and mESCs. Cells were incubated with 2 μM 5,5′,6,6′-tetrachloro-1,1′3,3′-tetraethyl-benzamidazol carboncyanine (JC-1) (**b**) or 10 μM 10-nonyl bromide (NAO) (**c**) for 30 min. JC-1 and NAO fluorescence levels were measured by flow cytometry at 480 and 550 nm, respectively. Data represent mean fluorescence ± s.d.

EB formation

mESCs were trypsinized to obtain a single mESC suspension, which was then transferred to uncoated Petri dishes (SPL Lifescience, Pocheon, Korea). The cells were cultured for 3 days in differentiation medium (high-glucose, glutamine-free Dulbecco's modified Eagle's medium) supplemented with 15% ES-qualified fetal bovine serum (HyClone, Logan, UT, USA), 2 mM GlutaMAX, 0.1 mM non-essential amino acid stock, 0.1 mM β-mercaptoethanol, 100 U ml^{-1} penicillin and 100 U ml^{-1} streptomycin).

Apoptosis levels

For cell apoptosis assays, cells were stained with Annexin V–fluorescein isothiocyanate and propidium iodide, and were evaluated for apoptosis by flow cytometry according to the manufacturer's protocol (BD PharMingen, San Diego, CA, USA).

Measurement of mitochondrial membrane potential

mESCs were trypsinized, collected and incubated with 5,5′,6,6′-tetrachloro-1,1′3,3′-tetraethyl-benzamidazol carboncyanine probe in 5 ml polystyrene, round-bottom tubes (Becton-Dickinson Biosciences, San Jose, CA, USA) for 15 min at 37 °C according to the manufacturer's specifications. The cells were then washed twice and analyzed with a FACSCalibur flow cytometer (excitation wavelength of 488 nm) (Becton-Dickinson Biosciences).

Determination of mitochondrial mass

mESCs were trypsinized and resuspended in 0.5 ml of phosphate-buffered saline containing 10 μM 10-nonyl bromide (Molecular Probes), which preferentially accumulates in mitochondria regardless of the mitochondrial membrane potential. After a 10 min incubation at 25 °C in the dark, cells were transferred immediately to a tube, incubated on ice and analyzed with a FACSCalibur flow cytometer (excitation wavelength of 550 nm).

RESULTS

Comparison of mitochondrial mass and function in MEFs and mESCs

To better understand structural and functional differences between the mitochondria of MEFs and mESCs, we began by evaluating their mitochondrial function and mass. We employed 5,5′,6,6′-tetrachloro-1,1′3,3′-tetraethyl-benzamidazol carboncyanine dye to estimate mitochondrial membrane potential and acridine orange 10-nonyl bromide to assess mitochondrial mass. We found that 5,5′,6,6′-tetrachloro-1,1′3,3′-tetraethyl-benzamidazol carboncyanine and 10-nonyl bromide fluorescence levels were decreased in mESCs compared with MEFs (Figures 1a and b), indicating that mitochondrial function and mass were reduced in mESCs compared with MEFs. Blue native-PAGE showed that the expression levels of electron transfer complexes II–IV, except for complex I, were slightly increased in mESCs compared with MEFs (Figure 1c). These data suggest that the decreased mitochondrial function in mESCs is mediated by other factors besides electron transfer complexes II–IV.

Increased expression of HSP60 in mESCs compared with MEFs

To determine whether the expression levels of proteins other than the electron transfer complexes differed between MEFs and mESCs, we performed two-dimensional electrophoresis analysis. We found that HSP60 and calnexin expression levels were higher in mESCs than in MEFs; in contrast, vimentin, transitional endoplasmic reticulum ATPase and ATP synthetase subunit-β expression levels were lower in mESCs compared with MEFs (Figure 2a). Of these, HSP60 expression showed the most prominent difference between MEFs and mESCs by two-dimensional electrophoresis. We further confirmed the increased expression of HSP60 in mESCs compared with MEFs at both the protein (Figure 2b) and mRNA (Figure 2c) levels. Finally, we determined that HSP60 was primarily located in the mitochondria in MEFs and mESCs (Figure 2d).

Depletion of HSP60 inhibits mESC proliferation and differentiation

To evaluate the role of HSP60 in mESCs, we depleted HSP60 using a doxycycline-inducible shRNA-expressing lentiviral vector. By western blotting, we showed that the HSP60-expressing lentiviral vector effectively decreased HSP60 expression levels in mESCs (Figure 3a). Notably, we found that HSP60 depletion resulted in decreased mitochondrial membrane potential and mass (Figures 3b and c), indicating a role

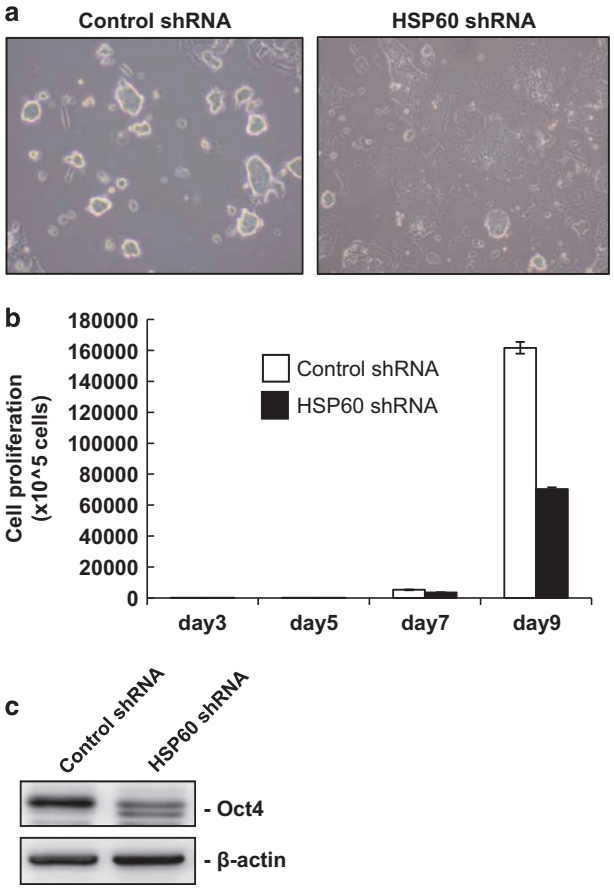

Figure 4 The effect of HSP60 knockdown on mESC proliferation. (**a**) mESC morphology 3 days after the induction of control or HSP60 shRNA expression. (**b**) Changes in the numbers of mESCs expressing control or HSP60 shRNA after 9 days. (**c**) OCT4 expression levels in mESCs expressing control or HSP60 shRNA after 2 days. OCT4 expression was analyzed by western blotting.

for HSP60 in the mitochondrial integrity of mESCs. In addition, HSP60 knockdown resulted in a decrease in the percentage of tightly packed cell colonies (Figure 4a). HSP60 knockdown also inhibited mESC proliferation by ~50% compared with that in control mESCs (Figure 4b). Moreover, depletion of HSP60 resulted in a split of the Oct4 protein band (47 and 43 kDa) (Figure 4c), suggesting that HSP60 knockdown affected OCT4 posttranslational modification. Furthermore, the sizes of EBs derived from HSP60-shRNA-expressing mESCs were smaller compared with mESCs expressing control shRNAs (Figures 5a and b). HSP60 knockdown also resulted in the increased expression of α-feto protein, an endoderm marker, but the decreased expression of brachyury, a mesoderm marker (Figures 5c and d). Taken together, these data indicate that HSP60 has an important role in mESC stemness and differentiation.

HSP60 knockdown enhances differentiation-induced apoptosis through AIF

It is well established that cell differentiation can lead to apoptotic cell death.[7,8] In addition, differentiated cells from mESCs undergo apoptosis.[9] We found that HSP60 knockdown decreased EB size and modulated EB-lineage specification (Figure 5). Thus, we examined whether HSP60 knockdown affects differentiation-induced apoptosis of mESCs. After 3 days of EB formation using the hanging drop culture method, we found that > 30% of cells were apoptotic (Figure 6a). Moreover, we showed that this HSP60 knockdown-induced increase in apoptosis was caspase-3 independent (Figure 6b). AIF is involved in initiating a caspase-independent pathway of apoptosis by causing DNA fragmentation and chromatin condensation.[7] Thus, we examined whether the effect of HSP60 on apoptosis is mediated by AIF. Notably, we found that depletion of AIF abolished the HSP60 knockdown-induced increase in differentiation-induced apoptosis of mESCs (Figures 6c and d), whereas HSP60 knockdown had no effect on MEF apoptosis (Figures 6e and f). HSP60 knockdown increased G2 phase cells in MEFs and S phase cells in mESCs (Figure 6g). Together, these data indicate that HSP60 has an important role in EB survival during differentiation.

DISCUSSION

ESC metabolism is heavily dependent on glycolysis, with 50–70% of glucose being converted to lactate.[10] ESCs are less reliant on oxidative phosphorylation compared with their differentiated counterparts and ESCs contain comparatively lower mitochondrial mass.[11] However, inhibition of oxidative phosphorylation affects self-renewal and the expression of pluripotency markers.[12] These findings indicate that oxidative phosphorylation is required for ES cell function, despite its utilization at reduced levels. In this study, we used proteomic analysis to better understand differences in mitochondrial protein levels between somatic cells and ESCs. We found that mitochondrial function and mass were reduced in mESCs compared with MEFs (Figures 1a and b). We also showed that the expression levels of electron transfer complexes I–IV did not differ between MEFs and mESCs (Figure 1c). Taken together, we conclude that, even though the function of the electron transport chain in ESC mitochondria is functionally intact, the ESC mitochondrial mass is lower in ESCs compared with somatic cells.

HSP60, also known as HSPD1 and chaperonin 60, is widely recognized as a molecular chaperone, with roles in cellular stress.[13] HSP60 is primarily located in mitochondria but has also been reported to be present in the cytoplasm.[14] HSP60 can act as either an inducer or inhibitor of apoptosis, depending on the conditions present.[15,16] In addition, HSP60 deficiency induces mitochondrial morphological aberrations and electrochemical potential collapse, indicating an important role for HSP60 in maintaining mitochondrial morphology and regulating mitochondrial activities.[17] However, its role in ESCs, which possess fewer mitochondria, remains largely unknown.

HSP60 knockdown in mESCs decreased the percentage of tightly packed cell colonies (Figure 4a), which is indicative of mESC differentiation. HSP60 knockdown also decreased EB size (Figure 5a). However, HSP60 knockdown mEBs are differentiated into three germ layer cells (Figures 5c and d).

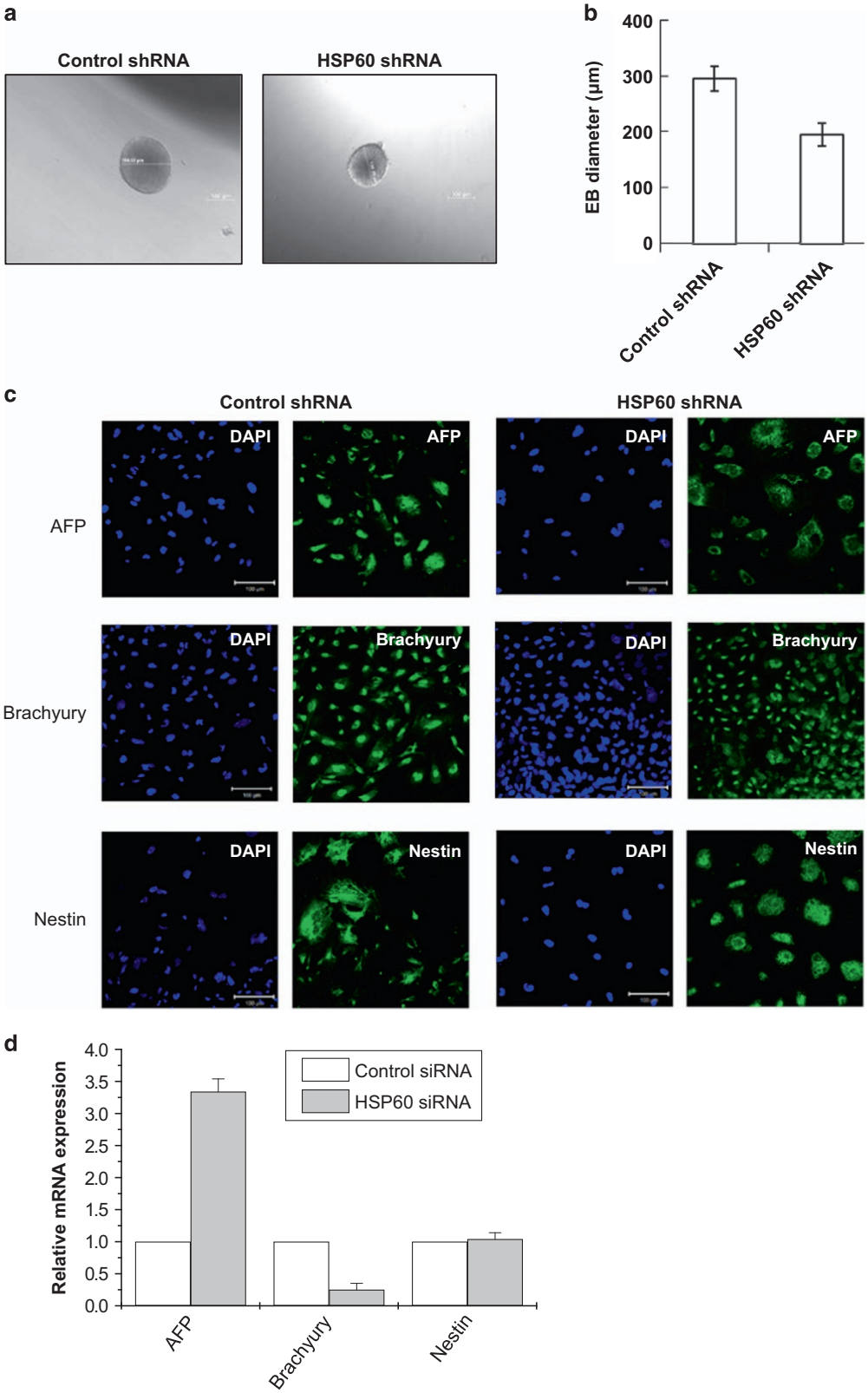

Figure 5 The effect of HSP60 knockdown on mESC differentiation. (**a**) The morphologies of EBs that were differentiated from control shRNA or HSP60 shRNA-expressing mESCs for 3 days. (**b**) The mean sizes of the embryoid bodies that were differentiated from control shRNA or HSP60 shRNA-expressing mESCs for 3 days. (**c**, **d**) The effects of HSP60 knockdown on the differentiation of mESCs into three germ layers. Control shRNA or HSP60 shRNA-expressing mESCs were spontaneously differentiated through embryoid body formation and were analyzed via immunocytochemistry (**c**) and real-time PCR (**d**) for lineage markers of the three embryonic germ layers (endoderm, α-feto protein (AFP); mesoderm, brachyury; and ectoderm, nestin).

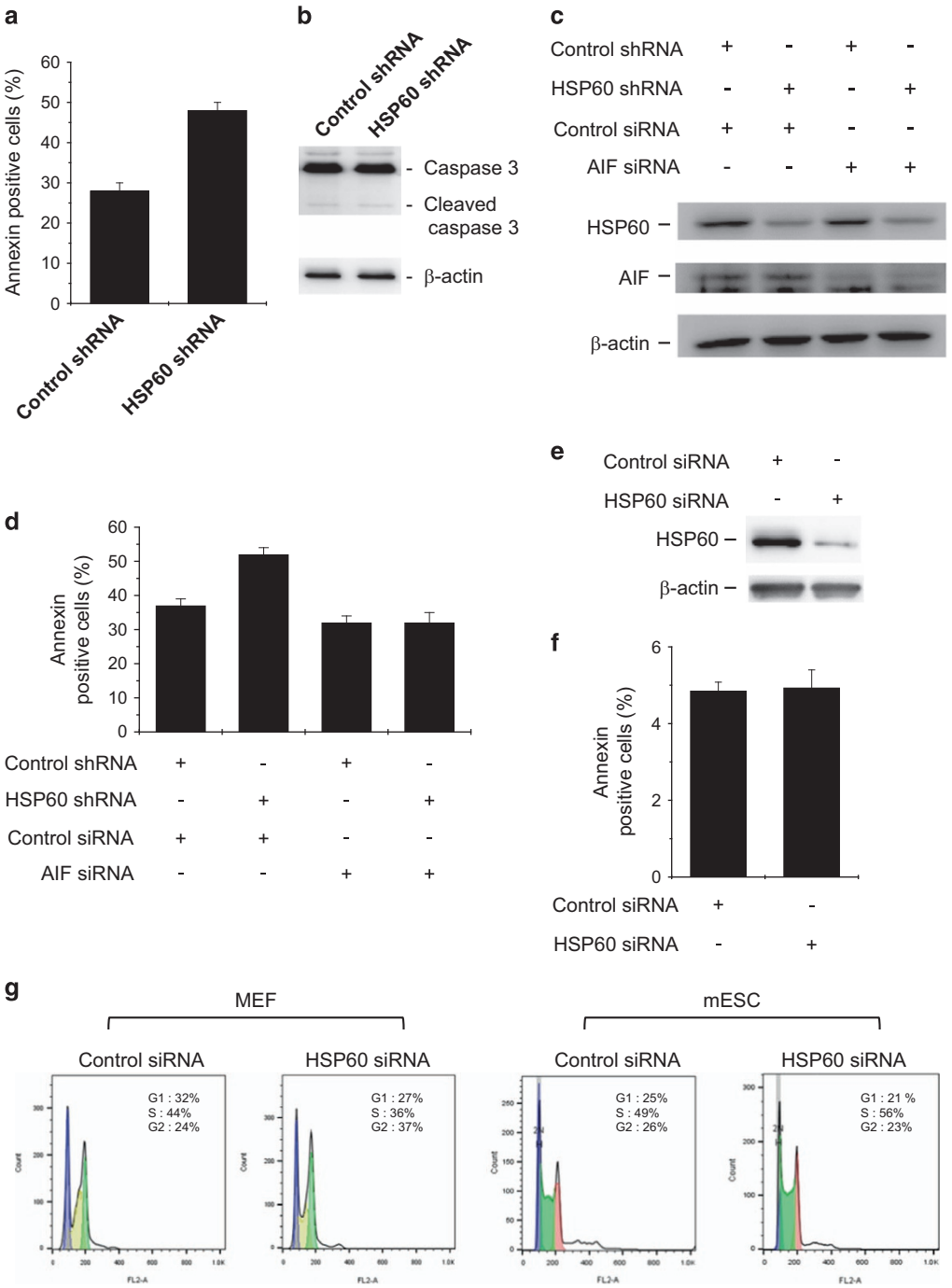

Figure 6 Effects of HSP60 and/or AIF knockdown on differentiation-induced apoptosis of mESCs. (**a**) Effect of HSP60 knockdown on differentiation-induced apoptosis. (**b**) Effect of HSP60 knockdown on caspase-3 activation. (**c**) HSP60 and/or AIF depletion in mESCs. Control shRNA or HSP60 shRNA-expressing mESCs were transfected with control or AIF small interfering RNA (siRNA) mESCs and cultured for 2 days. Protein expression levels were analyzed by western blotting. (**d**) Effects of HSP60 and/or AIF knockdown on differentiation-induced apoptosis. mESCs were differentiated into embryoid bodies for 3 days. The embryoid bodies were trypsinized and assayed for apoptosis levels using Annexin V. Data represent mean fluorescence ± s.d. (**e**, **f**) Effect of HSP60 depletion on MEF apoptosis. MEFs were transfected with control or HIF60 siRNA and cultured for 2 days. Protein expression levels were analyzed by western blotting (**e**). The cells were trypsinized and assayed for apoptosis levels using Annexin V. (**g**) Flow cytometry analysis of cell cycle distribution in MEFs and mESCs transfected with control or HSP60 siRNA for 48 h. Representative results of three separate experiments are shown, with the mean values of percentages of cells in G0/G1, S and G2/M.

HSP60 knockdown increases differentiation-induced apoptosis of mESCs (Figure 6). Taken together, HSP60 had a slight effect on differentiation and a marked effect on differentiation-induced apoptosis of mESCs, suggesting that HSP60 has a role in cell survival rather than differentiation.

In summary, we used an shRNA-mediated protein knockdown approach to examine the roles of HSP60 in mESCs. We found that HSP60 knockdown reduces mitochondrial mass and membrane potential in ESCs (Figure 3). HSP60 depletion also inhibits proliferation of mouse ESCs (Figures 4 and 5). Interestingly, HSP60 knockdown increases differentiation-induced apoptosis (Figure 6). This enhancement of apoptosis is caspase-independent and mediated by AIF. As one possible mechanism of action, inhibition of the HSP60 molecular chaperone functions to retain AIF in the cytosol, thereby mediating caspase-independent apoptosis. Taken together, we conclude that HSP60 is required for functional compensation of the reduced mitochondrial mass in mESCs and for cell survival during mESC differentiation.

CONFLICT OF INTEREST

The authors declare no conflict of interest.

ACKNOWLEDGEMENTS

This work was supported by the Bio & Medical Technology Development Program through NRF funded by the Ministry of Science, ICT and Future Planning (NRF-2012M3A9C6050363 and NRF-2012M3A9B4028749), and the Medical Research Center Program (NRF-2017R1A5A2015061).

PUBLISHER'S NOTE

Springer Nature remains neutral with regard to jurisdictional claims in published maps and institutional affiliations.

1 Thomson JA, Itskovitz-Eldor J, Shapiro SS, Waknitz MA, Swiergiel JJ, Marshall VS *et al.* Embryonic stem cell lines derived from human blastocysts. *Science* 1998; **282**: 1145–1147.
2 Nishikawa S, Jakt LM, Era T. Embryonic stem-cell culture as a tool for developmental cell biology. *Nat Rev Mol Cell Biol* 2007; **8**: 502–507.
3 Doss MX, Koehler CI, Gissel C, Hescheler J, Sachinidis A. Embryonic stem cells: a promising tool for cell replacement therapy. *J Cell Mol Med* 2004; **8**: 465–473.
4 Rafalski VA, Mancini E, Brunet A. Energy metabolism and energy-sensing pathways in mammalian embryonic and adult stem cell fate. *J Cell Sci* 2012; **125**: 5597–5608.
5 Varum S, Rodrigues AS, Moura MB, Momcilovic O, CAt Easley, Ramalho-Santos J *et al.* Energy metabolism in human pluripotent stem cells and their differentiated counterparts. *PLoS ONE* 2011; **6**: e20914.
6 Zhang J, Khvorostov I, Hong JS, Oktay Y, Vergnes L, Nuebel E *et al.* UCP2 regulates energy metabolism and differentiation potential of human pluripotent stem cells. *EMBO J* 2011; **30**: 4860–4873.
7 Cande C, Cecconi F, Dessen P, Kroemer G. Apoptosis-inducing factor (AIF): key to the conserved caspase-independent pathways of cell death? *J Cell Sci* 2002; **115**: 4727–4734.
8 Kim YS, Inui H, McMahon RJ. Ring opening of 2,5-didehydrothiophene: matrix photochemistry of C4H2S isomers. *J Org Chem* 2006; **71**: 9602–9608.
9 Duval D, Malaise M, Reinhardt B, Kedinger C, Boeuf H. A p38 inhibitor allows to dissociate differentiation and apoptotic processes triggered upon LIF withdrawal in mouse embryonic stem cells. *Cell Death Differ* 2004; **11**: 331–341.
10 Kondoh H, Lleonart ME, Nakashima Y, Yokode M, Tanaka M, Bernard D *et al.* A high glycolytic flux supports the proliferative potential of murine embryonic stem cells. *Antioxid Redox Signal* 2007; **9**: 293–299.
11 Cho YM, Kwon S, Pak YK, Seol HW, Choi YM, Park DJ *et al.* Dynamic changes in mitochondrial biogenesis and antioxidant enzymes during the spontaneous differentiation of human embryonic stem cells. *Biochem Biophys Res Commun* 2006; **348**: 1472–1478.
12 Mandal S, Lindgren AG, Srivastava AS, Clark AT, Banerjee U. Mitochondrial function controls proliferation and early differentiation potential of embryonic stem cells. *Stem Cells* 2011; **29**: 486–495.
13 Koll H, Guiard B, Rassow J, Ostermann J, Horwich AL, Neupert W *et al.* Antifolding activity of hsp60 couples protein import into the mitochondrial matrix with export to the intermembrane space. *Cell* 1992; **68**: 1163–1175.
14 Soltys BJ, Gupta RS. Immunoelectron microscopic localization of the 60-kDa heat shock chaperonin protein (Hsp60) in mammalian cells. *Exp Cell Res* 1996; **222**: 16–27.
15 Kirchhoff SR, Gupta S, Knowlton AA. Cytosolic heat shock protein 60, apoptosis, and myocardial injury. *Circulation* 2002; **105**: 2899–2904.
16 Shan YX, Liu TJ, Su HF, Samsamshariat A, Mestril R, Wang PH. Hsp10 and Hsp60 modulate Bcl-2 family and mitochondria apoptosis signaling induced by doxorubicin in cardiac muscle cells. *J Mol Cell Cardiol* 2003; **35**: 1135–1143.
17 Davis BA, Schwartz A, Samaha FJ, Kranias EG. Regulation of cardiac sarcoplasmic reticulum calcium transport by calcium-calmodulin-dependent phosphorylation. *J Biol Chem* 1983; **258**: 13587–13591.